Ab initio study of reaction of dimethyl sulfoxide (DMSO) with OH radical

ARTICLE *in* CHEMICAL PHYSICS LETTERS · APRIL 2002

Impact Factor: 1.9 · DOI: 10.1016/S0009-2614(02)00397-4

2 AUTHORS, INCLUDING:

Liming Wang
South China University of Technology
61 PUBLICATIONS **580** CITATIONS

SEE PROFILE

26 April 2002

ELSEVIER

Chemical Physics Letters 356 (2002) 490–496

CHEMICAL PHYSICS LETTERS

www.elsevier.com/locate/cplett

Ab initio study of reaction of dimethyl sulfoxide (DMSO) with OH radical

Liming Wang, Jingsong Zhang *

Department of Chemistry, University of California at Riverside, Riverside, CA 92521, USA

Received 13 December 2001; in final form 6 February 2002

Abstract

Gas-phase reaction of dimethyl sulfoxide (DMSO) with OH radical is investigated using ab initio calculations. The $CH_3S(O)OH + CH_3$ product channel has an overall negative reaction activation energy, and it could proceed by formation of an addition complex $(CH_3)_2S(O) \cdot OH$ and subsequent dissociation into $CH_3S(O)OH + CH_3$ via an energy barrier at −29.8 kJ/mol below DMSO + OH. The other two product channels, $CH_3S(O)CH_2 + H_2O$ and $CH_3SO + CH_3OH$, have energy barriers of 12.4 and 78.4 kJ/mol above DMSO + OH, respectively. The $CH_3S(O)OH + CH_3$ product channel is likely the dominant pathway in the DMSO + OH reaction. © 2002 Published by Elsevier Science B.V.

1. Introduction

Dimethyl sulfoxide (DMSO) has been identified as a reaction intermediate in atmospheric oxidation of dimethyl sulfuide (DMS) from both laboratory [1] and field studies [2–4]. In atmosphere, DMSO is produced mainly from the O_2 partial pressure dependent channel of the reaction of DMS with OH radical [5], and to some extent, from reactions of DMS with halogen oxide radicals (ClO, BrO, and IO) in the marine boundary layers [6,7].

Reaction of DMSO with OH has been investigated in both gas and liquid phases [8–12]. The gas-phase reaction is fast, with its rate coefficient being in the range of $5–10 \times 10^{-11}$ cm^3 molecule^{-1} s^{-1} [11] and on average about a quarter of the collision limit $\sim 3 \times 10^{-10}$ cm^3 molecule^{-1} s^{-1}; the reaction rate is also insensitive to the H-atom isotope effect [9]. A complex formation mechanism was proposed by Urbanski et al. [10] and the gas-phase reaction has the features typical of a reaction with a negative activation barrier [13]. Urbanski et al. [10] identified a nearly unit production of CH_3 radical by IR absorption, thus of methanesulfinic acid ($CH_3S(O)OH$, MSIA), in the absence of O_2 and NO_x, while Sorensen et al. [8] observed only less than 3% of production of MSIA in the presence of O_2 and NO_x based on ion chromatography measurements. In addition, formation of dimethyl sulfone ($DMSO_2$) was

* Corresponding author. Also at: Air Pollution Research Center, University of California, Riverside, CA 92521, USA. Fax: +1-909-787-4713.

E-mail address: jingsong.zhang@ucr.edu (J. Zhang).

0009-2614/02/$ - see front matter © 2002 Published by Elsevier Science B.V.
PII: S0009-2614(02)00397-4

observed to have a yield of $22 \pm 10\%$ in DMSO oxidation by OH radical in the air [11]. The discrepancy in the experimental MSIA yields could involve different fates of the reaction addition complex in the presence or absence of O_2 and the formation of $DMSO_2$ in DMSO oxidation by OH radical in the air.

To our knowledge, theoretical work on the reaction of DMSO with OH was not previously available, in contrast to the extensive studies of the DMS + OH reaction [14–18]. In this work, ab initio studies are reported on the reaction of DMSO with OH. Potential energy minima of the addition complexes and transition states of the reaction are located, and energetics of the reaction is examined. The reaction mechanism is analyzed based on the calculated results.

2. Computational methods

All ab initio calculations are carried out using GAUSSIAN 98 program [19]. Geometries of the stable species and transition states are fully optimized at MP2/6-311G(d,p) level of theory. Vibrational frequencies are obtained at the same level of theory for calculations of zero-point energies (ZPEs) and verifications of the optimized geometries. Transition states are characterized by one imaginary vibrational frequency associated with the reaction coordinate. Scaling factors of vibrational frequencies are 0.975 for ZPEs and 0.95 for comparison with experimental frequencies [20]. The optimized geometries are subjected to GAUSSIAN 3 (G3) single-point energy calculations [21]. Parameters for high-level correction (HLC) are chosen as those optimized from G3 calculations based on B3LYP/6-31G(d) geometries and ZPEs [22]. The energy calculations are approximately at the QCISD(T)/G3Large level of theory with full electron correlation, with a standard deviation of ~4 kJ/mol for enthalpies of reactions and ~8 kJ/mol for energies of transition states [23,24]. All energy calculations here are at this level unless otherwise stated.

Spin contamination of open-shell systems in this study is small. For stationary radicals, expectation values of the total spin $\langle S^2 \rangle$ are <0.78 before spin annihilation in all the calculations, and <0.76 after spin annihilations. For transition states, spin contamination is larger than in stable radicals; however, all the values of $\langle S^2 \rangle$ are less than 0.77 after spin annihilations. GAUSSIAN 3 has been shown to have good performance on the radical reactions with relatively large spin contaminations [25].

As the basis set effect is an important issue in geometric optimization of sulfur-containing species [26–28], geometries of DMSO, $DMSO_2$, MSIA, and CH_3SO are also optimized by MP2 with larger cc-pVTZ basis sets [29]. The optimized geometries with MP2/6-311G(d,p) and MP2/cc-pVTZ agree within 0.02 Å in bond lengths and 1.0° in bond angles, and the MP2/cc-pVTZ geometries have slightly lower energies than the MP2/6-311G(d,p) ones with energy differences within 2 kJ/mol. In general, the 6-311G(d,p) basis sets are adequate in this study.

3. Results and discussions

There are four exothermic product channels in the DMSO + OH reaction (Table 1):

$$CH_3S(O)CH_3 + OH \rightarrow (CH_3)_2S(O)\text{–}OH \quad (1a)$$
$$\rightarrow CH_3S(O)OH + CH_3 \quad (1b)$$
$$\rightarrow CH_3S(O)CH_2 + H_2O \quad (1c)$$
$$\rightarrow CH_3SO + CH_3OH \quad (1d)$$

The adduct formation (1a) could be an intermediate step for the S–C bond breaking (1b) or H-abstraction (1c). Channel (1d) is expected to have an SN2-type transition state with the CH_3 group inverted during the reaction. The optimized geometries of reactants and products are shown in Fig. 1, addition complexes in Fig. 2, and transition states in Fig. 3. The calculated enthalpies and activation energies of reactions, and vibrational frequencies are listed in Tables 1 and 2, respectively.

3.1. Addition complexes of DMSO with OH

The Lewis structure of DMSO can be viewed as $(CH_3)_2S^+\text{–}O^-$, with strongly charged S and O atoms, which shorten the S–O bond lengths by

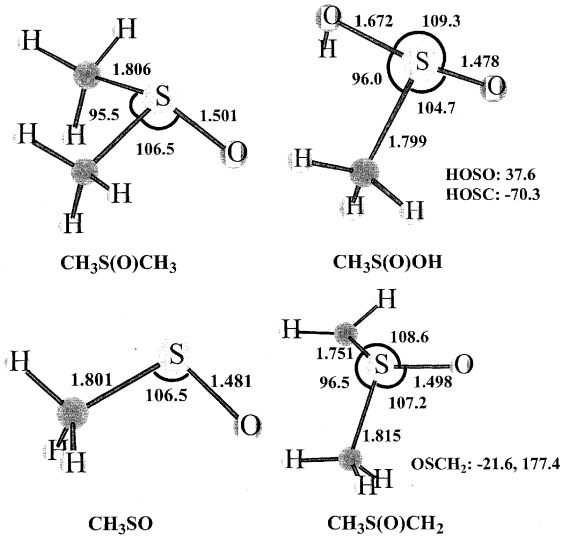

Fig. 1. Optimized geometries of sulfur-containing species at MP2/6-311G(d,p) level of theory. Bond lengths are in angstroms and angles are in degrees.

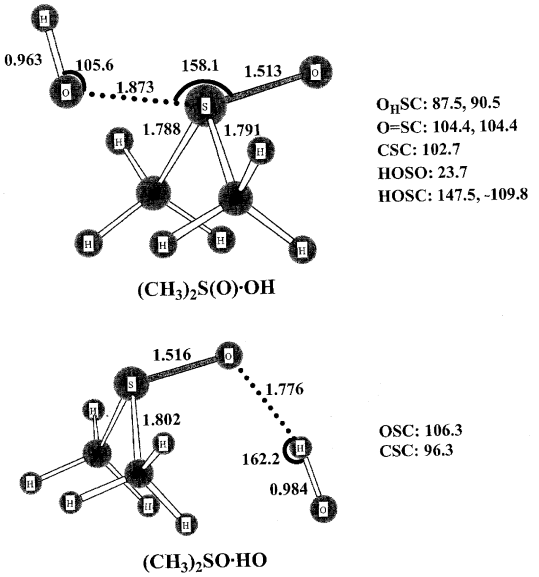

Fig. 2. Geometries of addition complexes between $CH_3S(O)CH_3$ and OH. See text for more details.

Coulomb interaction. This is common in sulfoxides, e.g., 1.501 Å of S–O in DMSO and 1.478 Å of S–O in $CH_3S(O)OH$, while the single bond S–OH in $CH_3S(O)OH$ is 1.672Å (Fig. 1).

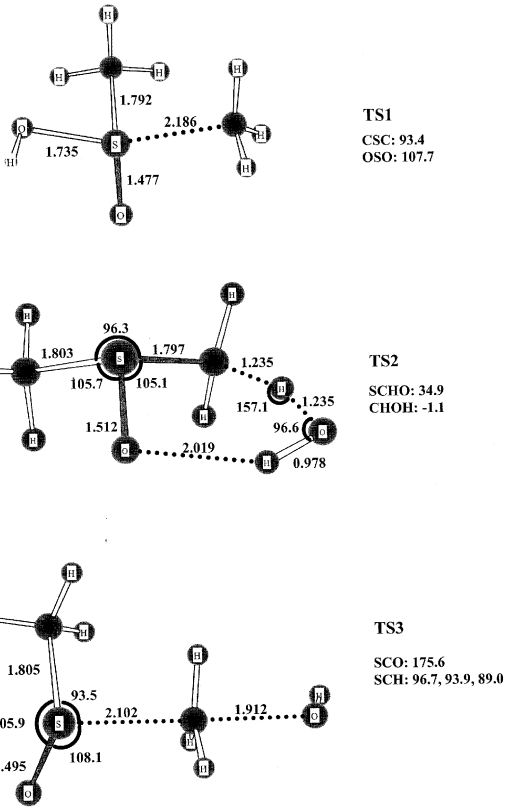

Fig. 3. Geometries of transition states of the DMSO + OH reaction.

Because of the lone-electron pair on sulfur and the highly polarized S–O bond, two types of addition complexes of DMSO with the OH radical are possible (Fig. 2): (i) a $(CH_3)_2S(O) \cdot OH$ adduct formed via a 2-center-3-electron (2c–3e) bond due to the sulfur-lone-electron pair; and (ii) a $(CH_3)_2SO \cdot HO$ complex formed via hydrogen-bond between the negatively charged O-atom and HO, and via dipole–dipole interaction between DMSO and OH. This situation is similar to that in the DMS–OH system [15–18]. No stable $CH_3S(O)CH_2$–H · OH complex is found; its geometrical optimizations at MP2/6-311G(d,p) level either end up with one of the two addition complexes mentioned above, or fall apart to the DMSO + OH reactants.

The binding energy of $(CH_3)_2SO \cdot HO$ is calculated to be 46.6 kJ/mol at 0 K and 50.7 kJ/mol at

Table 1
Enthalpy changes and activation energies of reactions (in kJ/mol) calculated at G3 + ZPE // MP2/6-311G(d,p) level of theory

Reactions		$\Delta_r H_0^\circ$	$\Delta_r H_{298}^\circ$	E_a (0 K)
$CH_3S(O)CH_3 + OH \rightarrow (CH_3)_2S(O)\cdot OH$	(1a)	−46.6	−50.7	
$CH_3S(O)CH_3 + OH \rightarrow (CH_3)_2SO\cdot HO$	(1a)	−30.7	−33.7	
$CH_3S(O)CH_3 + OH \rightarrow CH_3S(O)OH + CH_3$	(1b)	−68.0	−66.1	−29.8
$CH_3S(O)CH_3 + OH \rightarrow CH_3S(O)CH_2 + H_2O$	(1c)	−64.5	−63.6	12.4
$CH_3S(O)CH_3 + OH \rightarrow CH_3SO + CH_3OH$	(1d)	−242.6	−244.1	78.4
$(CH_3)_2S(O)\cdot OH + O_2 \rightarrow CH_3S(O)_2CH_3 + HO_2$	(2)	−186.5	−188.5	
$CH_3S(O)OH \rightarrow CH_3SO + OH$		193.0	198.9	

ZPE scale factor is 0.975.

Table 2
Vibrational frequencies of sulfur-containing species at the MP2/6-311G(d,p) level of theory

Species	Vibrational frequencies (in cm^{-1}, scaled by 0.95)
$CH_3S(O)CH_3$	150, 231, 283, 300, 357, 661, 681, 862, 896, 933, 989, 1067, 1284, 1309, 1379, 1395, 1396, 1414, 2926, 2928, 3034, 3037, 3042, 3044
$CH_3S(O)_2CH_3$	171, 214, 265, 285, 350, 441, 462, 675, 732, 898, 920, 962, 977, 1114, 1302, 1303, 1320, 1386, 1396, 1402, 1407, 2946, 2949, 3055, 3056, 3062, 3066
$CH_3S(O)OH$	225, 246, 310, 396, 421, 669, 698, 914, 921, 1064, 1158, 1303, 1385, 1399, 2931, 3037, 3054, 3589
$CH_3S(O)CH_2$	134, 219, 276, 310, 340, 468, 657, 701, 860, 915, 936, 1071, 1291, 1351, 1386, 1405, 2933, 3034, 3045, 3049, 3172
CH_3SO	155, 328, 687, 854, 917, 1267, 1302, 1383, 1401, 2929, 3034, 3038
$(CH_3)_2S(O)\cdot OH$	120, 146, 172, 219, 309, 319, 347, 367, 527, 687, 749, 873, 905, 936, 961, 998, 1069, 1300, 1322, 1390, 1391, 1402, 1406, 2950, 2954, 3054, 3060, 3080, 3085, 3679
$(CH_3)_2SO\cdot HO$	60, 102, 172, 215, 250, 287, 304, 374, 576, 670, 695, 761, 879, 908, 942, 1004, 1035, 1287, 1319, 1379, 1401, 1401, 1421, 2932, 2933, 3041, 3044, 3047, 3048, 3348
$DMSO + OH \rightarrow CH_3S(O)OH + CH_3$*	393*i*, 112, 146, 180, 214, 290, 324, 355, 425, 611, 616, 657, 733, 924, 937, 1013, 1034, 1140, 1305, 1367, 1376, 1395, 1398, 2949, 2955, 3059, 3069, 3106, 3113, 3650
$DMSO + OH \rightarrow CH_3S(O)CH_2 + H_2O$*	2149*i*, 51, 155, 214, 262, 308, 333, 382, 522, 653, 679, 694, 857, 898, 928, 960, 1008, 1049, 1138, 1297, 1354, 1386, 1407, 1476, 2929, 2969, 3041, 3044, 3072, 3489
$DMSO + OH \rightarrow CH_3SO + CH_3OH$*	1524*i*, 93, 117, 132, 169, 205, 258, 301, 329, 357, 676, 842, 897, 922, 974, 1019, 1066, 1109, 1301, 1327, 1351, 1383, 1403, 2927, 2980, 3034, 3041, 3163, 3183, 3667

* Transition states of the reactions.

298 K. This binding energy is slightly larger than that in the 2c–3e DMS–OH complex (31.1 kJ/mol at 0 K at G2//B3LYP/cc-pVTZ [18], 37.5 kJ/mol at 298 K at G2++(UMP2)//B3LYP/6-31++G(2d,p), 34.5 kJ/mol at 298 K at G2++(UMP2)//UMP2 (Full)/6-31++G(2d,p) [17], and 44.8 ± 10.5 kJ/mol between DMS-d_6 and OH from experimental study [30]). At the MP2/6-311G(d,p) level of theory, the S–OH bond length in $(CH_3)_2S(O)\cdot OH$ is 1.873 Å, comparable to that of a S–O single bond, e.g., 1.672 Å in MSIA. This bond length is much shorter than that in the DMS–OH complex (2.047 Å at MP2/6-31+G(2d) level of theory [15]). The shortening of the S–OH bond length from $(CH_3)_2S\cdot OH$ to $(CH_3)_2S(O)\cdot OH$ is also identified in B3LYP/cc-pVTZ calculations (from 2.326 to 2.085 Å [18]). The vibrational frequency of the S–OH stretch in $(CH_3)_2S(O)\cdot OH$ is 527 cm^{-1}, comparable to 669 cm^{-1} of the S–OH stretch in $CH_3S(O)OH$. Note that there is a significant charge transfer of ~0.4*e* from DMSO to OH in this 2c–3e complex.

The binding energy of $(CH_3)_2SO\cdot HO$ is 30.7 kJ/mol at 0 K and 33.7 kJ/mol at 298 K, approximately 17 kJ/mol lower than that of $(CH_3)_2S(O)\cdot OH$. This complex is characterized by the strong hydrogen bond between O-atom in DMSO and the HO radical, along with the dipole–dipole

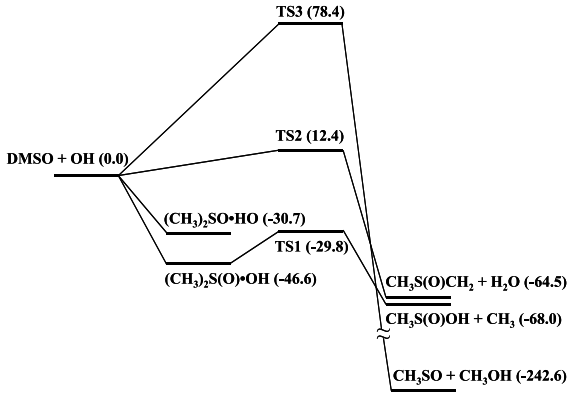

Fig. 4. Energy level diagram of the DMSO + OH reaction. Energies are at 0 K and in kJ/mol.

interaction between DMSO and OH, and possibly the hydrogen bonds between O_{HO}–H_3C_{DMSO} as in the DMSO–OH^- complex [31]. While the last term is small due to the large O–H_3C separation (>2.6 Å), the hydrogen bonding between HO and O_{DMSO} contributes the most to the stability of the $(CH_3)_2SO \cdot HO$ complex. The O–H bond length of 1.776 Å is typical for a hydrogen bond of medium strength [32]. The vibrational frequency of the O–HO stretch in the complex is 215 cm^{-1}. The binding energy of $(CH_3)_2SO \cdot HO$ is large than that in the H-bonding DMS–OH complex (15.5 kJ/mol at 0 K by G2) [18].

The addition complex $(CH_3)_2S(O) \cdot OH$ could further react with O_2 to produce $DMSO_2$

$$(CH_3)_2S(O) \cdot OH + O_2 \rightarrow CH_3S(O)_2CH_3 + HO_2 \quad (2)$$

which might be the mechanism of $DMSO_2$ formation in atmospheric oxidation of DMSO [11]. This reaction is exothermic, with the calculated $\Delta_r H_0^\circ = -186.5$ kJ/mol and $\Delta_r H_{298}^\circ = -188.5$ kJ/mol; further study is needed to locate its transition state and reaction barrier.

3.2. Transition states

The enthalpies of reaction of the three exothermic reaction channels (1b)–(1d) are −68.0, −64.5, and −242.6 kJ/mol (at 0 K), respectively. Their transition states are depicted in Fig. 3 as **TS1**, **TS2**, and **TS3**. Energy diagram of the DMSO + OH system is shown in Fig. 4.

The transition state (**TS1**, Fig. 3) of the $CH_3S(O)OH + CH_3$ channel (1b) can be evolved from the $(CH_3)_2S(O) \cdot OH$ adduct. **TS1** is 16.8 kJ/mol above $(CH_3)_2S(O) \cdot OH$, but −29.8 kJ/mol (at 0 K) below DMSO + OH. **TS1** has a large bond distance between the S-atom and the departing CH_3 group (2.186 Å) and a product-like $CH_3S(O)OH$ moiety. The forming S–OH bond is 1.735 Å (only slightly longer than 1.672 Å in the $CH_3S(O)OH$ product). These features are similar to those in the reaction between DMS and OH [18]. The structure of **TS1** indicates a late barrier and a tight ($\Delta S^{\neq} < 0$) transition state for this exothermic S–C bond breakage channel (1b).

The transition state (**TS2**, Fig. 3) of H-abstraction channel (1c) has a 5-member ring, in which the hydrogen bonding is formed to facilitate the reaction by lowering the energy barrier. The addition complex $(CH_3)_2SO \cdot HO$ might be a reaction intermediate for this channel. **TS2** is above $(CH_3)_2SO \cdot HO$ by 43.1 kJ/mol and above DMSO + OH by 12.4 kJ/mol. In **TS2**, both the forming OH bond and the breaking C–H bond are 1.235 Å. A late barrier is located in **TS2**. The OH radical approaches the H-atom from above the OSC plane, with the forming CH_2 group twisted to allow the lone pair on sulfur to stabilize the developing CH_2 radical center. The energy barrier of the H-abstraction reaction channel is close to that in the DMS + OH reaction (10.6 kJ/mol at 0 K with UMP2(full)/6-31+G(d) calculations [15]). Although the $CH_3S(O)CH_2$ radical product has been identified in the reaction of DMSO with OH in solution [12], channel (1c) should be less favored in the gas-phase compared to channel (1b).

An SN2-type transition state, **TS3**, is located for the reaction channel (1d). **TS3** has an almost linear S–C–O configuration (Fig. 3), with a broken S–C bond (2.102 Å), an elongated CH_3–OH bond (1.912 Å), and a nearly inverted CH_3 group (S–C–H angles range from 89° to 96°). The energy barrier of **TS3** relative to DMSO + OH is 78.4 kJ/mol. Channel (1d) would be the least likely channel despite of its largest exothermicity (−242.6 kJ/mol at 0 K). The energetic calculations are consistent with the experimental observation that no

CH_3OH production has been detected. It should be pointed out that spin contamination for post-Hartree–Fock calculations (MP2, MP4, and QCISD(T)) is severe for **TS3**. The $\langle S^2 \rangle$ value is $\sim$0.95 before, and $<$0.77 after spin-annihilation. Although the calculated energy of **TS3** is lifted by the spin contamination, the energy barrier is still much higher than those in reaction channels (1b) and (1c).

3.3. Gas-phase reaction mechanism

As shown in Fig. 4, the MSIA + CH_3 channel (1b) has an overall negative activation energy with respect to the DMSO + OH reactants and should dominate. This is consistent with the slightly negative temperature dependence of the reaction rate observed in a limited temperature range [9]. The H-abstraction channel (1c) is less important, and the $CH_3SO + CH_3OH$ channel (1d) is not possible at atmospheric temperature.

The reaction of DMSO with OH could proceed via the addition of OH to DMSO. In atmospheric environment, the $(CH_3)_2S(O) \cdot OH$ addition complex can undergo S–C bond breakage through **TS1** (which is below the initial reactants DMSO+OH), or further react with O_2. Based on the relative energetics, forward reaction to the S–C dissociation is much more likely than the backward decomposition of the complex to the reactants. The channel (1b) would be the predominant pathway in the reaction of DMSO with OH if the addition complex does not further react. This conclusion is consistent with the nearly unit production of CH_3 radical in the absence of O_2 [10] and isotopic identity of the hydrogen atoms, i.e., DMSO or DMSO-d_6 [9]. On the other hand, considerable amount of $DMSO_2$ production (with a yield of $22 \pm 10\%$) has been observed in the DMSO + $OH + O_2$ reaction [11], presumably due to the reaction of addition complex $(CH_3)_2S(O) \cdot OH$ with O_2 (reaction (2)). Thus, the dissociation lifetime of the addition complex must be long enough to allow its secondary collision with O_2 to produce $DMSO_2$ (at a collision frequency of $\sim 10^{10}$ s^{-1} at 10^5 Pa and 298 K and with a typical sum of molecular radii of 5 Å), i.e., the rate for adduct reaction with O_2 should be on the same order of magnitude of its dissociation reaction. It can also be inferred that the H-abstraction of $(CH_3)_2S(O) \cdot OH$ by O_2 is near the collision limit, and this fast H-abstraction might be due to the strong S–OH bond in the addition complex.

It is interesting to compare the DMSO + OH and DMS + OH reactions. Reaction of DMSO with OH proceeds via formation of the addition complex. The main reaction pathways are dissociation of the DMSO–OH complex into the MSIA + CH_3 products (as the energy barrier to this product channel is well below DMSO + OH) or further reaction with O_2; decomposition back to DMSO + OH reactants is very unlikely. On the other hand, the reaction pathways in the reaction of DMS with OH are H-abstraction from methyl group and formation of the addition complex DMS–OH. The H-abstraction channel has an energy barrier of only 10.6 kJ/mol [15], and is the major channel. The DMS–OH complex has an energy barrier of $\sim$30 kJ/mol (relative to DMS + OH) to dissociate into the $CH_3SOH + CH_3$ products [18], therefore the complex could decompose back to the DMS + OH reactants or be stabilized by third-body collisions, and an equilibrium between the reactants and addition complex can be established [1]. Adding O_2 to the DMS + OH system would deplete the DMS–OH complex due to the reaction between O_2 and the DMS–OH complex; hence an O_2-pressure dependence was observed in the DMS + OH reaction.

Acknowledgements

We acknowledge supports from San Diego Supercomputer Center, National Science Foundation (CHE-0111635), the Camille and Henry Dreyfus Foundation, and the Alfred P. Sloan Foundation.

References

[1] A.A. Turnipseed, S.B. Barone, A.R. Ravishankara, J. Phys. Chem. 100 (1996) 14703.
[2] D. Davis, G. Chen, P. Kasibhatla, A. Jefferson, D. Tanner, F. Eisele, D. Lenschow, W. Neff, H. Berresheim, J. Geophys. Res. Atmos. 103 (1998) 1657.

[3] G. Chen, D.D. Davis, P. Kasibhatla, A.R. Bandy, D.C. Thornton, B.J. Huebert, A.D. Clarke, B.W. Blomquist, J. Atmos. Chem. 37 (2000) 137.
[4] J.B. Nowak, D.D. Davis, G. Chen, F.L. Eisele, R.L. Mauldin, D.J. Tanner, C. Cantrell, E. Kosciuch, A. Bandy, D. Thornton, A. Clarke, Geophys. Res. Lett. 28 (2001) 2201.
[5] A.R. Ravishankara, Y. Rudich, R. Talukdar, S.B. Barone, Philos. Trans. R. Soc. London B 352 (1997) 171.
[6] T. Ingham, D. Bauer, R. Sander, P.J. Crutzen, J.N. Crowley, J. Phys. Chem. A 103 (1999) 7199.
[7] G.P. Knight, J.N. Crowley, Phys. Chem. Chem. Phys. 3 (2001) 393.
[8] S. Sorensen, H. Falbehansen, M. Mangoni, J. Hjorth, N.R. Jensen, J. Atmos. Chem. 24 (1996) 299.
[9] A.J. Hynes, P.H. Wine, J. Atmos. Chem. 24 (1996) 23.
[10] S.P. Urbanski, R.E. Stickel, P.H. Wine, J. Phys. Chem. A 102 (1998) 10522.
[11] H. Falbe-Hansen, S. Sorensen, N.R. Jensen, T. Pedersen, J. Hjorth, Atmos. Environ. 34 (2000) 1543.
[12] J.R. Woodward, T.S. Lin, Y. Sakaguchi, H. Hayashi, J. Phys. Chem. A 104 (2000) 557.
[13] S.W. Benson, O. Dobis, J. Phys. Chem. A 102 (1998) 5175.
[14] M. Gu, F. Turecek, J. Am. Chem. Soc. 114 (1992) 7146.
[15] M.L. McKee, J. Phys. Chem. 97 (1993) 10971.
[16] F. Turecek, J. Phys. Chem. 98 (1994) 3701.
[17] F. Turecek, Collect Czech. Chem. Commun. 65 (2000) 455.
[18] L.M. Wang, J.S. Zhang, J. Mol. Struct. Theochem. 543 (2001) 167.
[19] M.J. Frisch et al. GAUSSIAN 98 A.7, 1998.
[20] A.P. Scott, L. Radom, J. Phys. Chem. 100 (1996) 16502.
[21] L.A. Curtiss, K. Raghavachari, P.C. Redfern, V. Rassolov, J.A. Pople, J. Chem. Phys. 109 (1998) 7764.
[22] A.G. Baboul, L.A. Curtiss, P.C. Redfern, K. Raghavachari, J. Chem. Phys. 110 (1999) 7650.
[23] D.K. Malick, G.A. Petersson, J.A. Montgomery, J. Chem. Phys. 108 (1998) 5704.
[24] T.P.W. Jungkamp, J.H. Seinfeld, J. Chem. Phys. 107 (1997) 1513.
[25] C.J. Parkinson, P.M. Mayer, L. Radom, J. Chem. Soc. Perkin Trans. 2 (1999) 2305.
[26] S.S. Xantheas, T.H. Dunning, J. Phys. Chem. 97 (1993) 6616.
[27] B.A. Smart, C.H. Schiesser, J. Comput. Chem. 16 (1995) 1055.
[28] P.J.A. Ruttink, P.C. Burgers, J.T. Francis, J.K. Terlouw, J. Phys. Chem. 100 (1996) 9694.
[29] D.E. Woon, T.H. Dunning, J. Chem. Phys. 98 (1993) 1358.
[30] S.B. Barone, A.A. Turnipseed, A.R. Ravishankara, J. Phys. Chem. 100 (1996) 14694.
[31] P. Burk, U. Molder, I.A. Koppel, A. Rummel, A. Trummal, J. Phys. Chem. 100 (1996) 16137.
[32] G.A. Jeffery, An Introduction to Hydrogen Bonding, Oxford University Press, New York, 1997.